A New Monoclinic Perovskite Allotype in $Pr_{0.6}Sr_{0.4}MnO_3$

C. Ritter and P. G. Radaelli

Institut Laue-Langevin, B.P. 156, Grenoble Cedex 09, France

and

M. R. Lees, J. Barratt, G. Balakrishnan, and D. McK. Paul

Department of Physics, University of Warwick, Coventry CV4 7AL, United Kingdom

We report the observation, in $Pr_{0.6}Sr_{0.4}MnO_3$, of a low-temperature phase transition between *Pnma* and the monoclinic space group *I2/a*. The *I2/a* allotype has never previously been observed in the $(R_{1-x}A_x)MnO_3$ manganese perovskite system. Furthermore, this space group symmetry is not present in the recently published phase diagram obtained at 30% Mn^{+4}, indicating that electronic doping has a direct effect on the phase stability. The structural and magnetic parameters for the new phase, as obtained from Rietveld refinements of neutron powder diffraction data, are also reported. © 1996 Academic Press

1. INTRODUCTION

The discovery of giant or colossal magnetoresistance (CMR) has stimulated a renewed interest in distorted manganese perovskites of type $(R_{1-x}A_x)MnO_3$, where R stands for a rare earth or La and A for a divalent alkali metal. Based on the pioneering work of Wollan and Koehler (1) who examined the $La_{1-x}Ca_xMnO_3$ system, and on the work of Jirák *et al.* (2–5) who studied the $Pr_{1-x}A_xMnO_3$ series with A = Ca, Sr, Ba, much effort has been devoted to the study of the magnetic and structural properties of these compounds, aiming at a better understanding of CMR.

With the parent compounds $LaMnO_3$ and $PrMnO_3$ being *A*-type antiferromagnets (due to the antiferromagnetic superexchange interaction), it is well accepted by now that the substitution of the trivalent rare earth by the divalent alkali metal leads to the formation of Mn^{4+} and, through the double exchange mechanism, to ferromagnetic interactions (6).

Depending on the ionic radius of the alkali and the nature of the rare earth, a number of different types of behavior are observed. $La_{1-x}Ca_xMnO_3$ and $La_{1-x}Sr_xMnO_3$ $(0.1 \leq x \leq 0.4)$ are ferromagnetic, with conductivities which are semiconductor-like above T_C and metallic below T_C.

The largest magnetoresistance ratios were found for compounds around the 33% substitution level (7–10). $Pr_{1-x}Sr_xMnO_3$ $(0.2 \leq x \leq 0.5)$ is also ferromagnetic with metallic behavior below T_C. However, for Ca or Sr concentrations of around 50%, the conducting/ferromagnetic state is replaced at lower temperatures by a charge-ordered/antiferromagnetic state, where resistivity exhibits activated behavior (11). The application of a magnetic field can melt the charge ordered lattice and lead to the restoration of a conducting/ferromagnetic regime. In the case of $Pr_{1-x}Ca_x$ MnO_3 $(0.3 \leq x \leq 0.45)$, the magnetic and charge ordering transitions occur at different temperatures (2, 12, 13). Below the charge ordering temperature, the application of a sufficiently high magnetic field induces a transition from either a paramagnetic or antiferromagnetic state into a ferromagnetically ordered state. This transition is accompanied by a decrease in the resistivity of the material and, at low temperature, this results in a field induced insulator–metal transition.

It is presently being discussed whether the double exchange mechanism alone is able to explain the behavior of this range of materials, or if additional mechanisms are required (14).

Studying the temperature dependence of the small angle scattering intensity seen by neutron diffraction in $La_{2/3}$ $Ca_{1/3}MnO_3$, De Teresa *et al.* (15) explained, for instance, the dramatic effect of T_C using the idea of magnetic polarons already introduced by Kusters *et al.* (7) in their original paper. On the other hand, Millis and co-workers have emphasized the importance of lattice distortions in general, and Jahn–Teller distortions of the MnO_6 octahedra around Mn^{+3} in particular, as essential elements in describing the physics of these compounds (14, 16).

In addition to the electronic doping, it is now well established that the average size of the cations on the *A*-site is a critical factor in determining both structural and electronic

276

properties of perovskite manganites. Hwang *et al.* (17) and Radaelli *et al.* (18) proposed a scheme where at constant doping level ($x = 0.3$) the temperature dependent magnetic and structural behavior of differently substituted systems could be well classified using the notion of the tolerance factor as introduced by Goldschmidt (19). They related the observed change of the transport and magnetic properties as a function of the tolerance factor to the Mn–Mn electron hopping parameter which is determined by the Mn–O–Mn bond angle. Referring to the diagram of Hwang *et al.,* the absence of a temperature induced insulator–metal transition as found, for instance, in $(Tb_{1/3}La_{2/3})_{2/3}Ca_{1/3}MnO_3$ (Ref. 20) can be associated with the absence of long-range ferromagnetic order in this compound where, due to the small size of Tb^{3+}, the tolerance factor is lower than a critical value.

The work of Hwang *et al.* and Radaelli *et al.* concentrated on the 0.3 doping level and it is unclear to what extent the conclusions valid for this substitution level can be transferred to different doping levels at least as far as the structural phase diagram is concerned. In fact, even at constant tolerance factor, we may expect that structural parameters which are directly controlled by the doping level, such as the Jahn–Teller distortion of the MnO_6 octahedra, may have an influence on the relative stability of the various perovskite allotypes. The following question can therefore be asked: is the tolerance factor the only parameter determining the *structural* properties of the $RMnO_3$ phases?

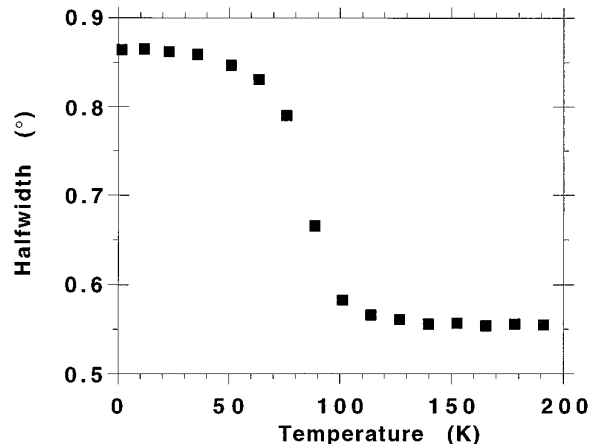In order to answer this question, we measured several

FIG. 2. The halfwidth of the 121/200/002 reflection as a function of temperature (based on D1B data).

samples of the $PrSrCaMnO_3$ system, all at the $x = 0.4$ doping level. The results of our systematic temperature dependent studies will be presented elsewhere. In this paper, we concentrate on the discovery of a new monoclinic phase found at low temperatures for $Pr_{0.6}Sr_{0.4}MnO_3$. The study will show that for a doping level not too different from that studied by Radaelli *et al.,* the structural phase diagram already includes a different low-temperature phase. This observation implies that, for these compounds, electronic doping has a direct effect on the structural phase diagram.

2. SAMPLE PREPARATION AND EXPERIMENTAL DETAILS

A polycrystalline sample of $Pr_{0.6}Sr_{0.4}MnO_3$ was prepared by a normal solid state reaction route. Stoichiometric quantities of Pr_6O_{11}, $SrCO_3$, and MnO_2 were repeatedly ground and then sintered in air for 12 h at a temperature of 1350°C before finally being pressed into pellets and sintered at the same temperature for 24 h.

Neutron diffraction data were collected at the Institute Laue–Langevin, initially on the D1B high intensity 2 axis diffractometer using a wavelength of $\lambda = 2.52$ Å. D1B is equipped with a 400 cell one-dimensional multidetector covering 80° in 2Θ. The sample was placed inside a vanadium cylinder and measured in an orange cryostat between 1.6 and 320 K. High resolution data were subsequently collected with the D2B diffractometer at five temperatures in the high intensity mode, using a wavelength of 1.594 Å. At 1.6 K, an additional data set was obtained at $\lambda = 2.39$ Å, using a secondary collimation $\alpha_2 = 0.2°$, in order to further enhance the resolution. Structural parameters were refined by the Rietveld method using the FULLPROF program (21).
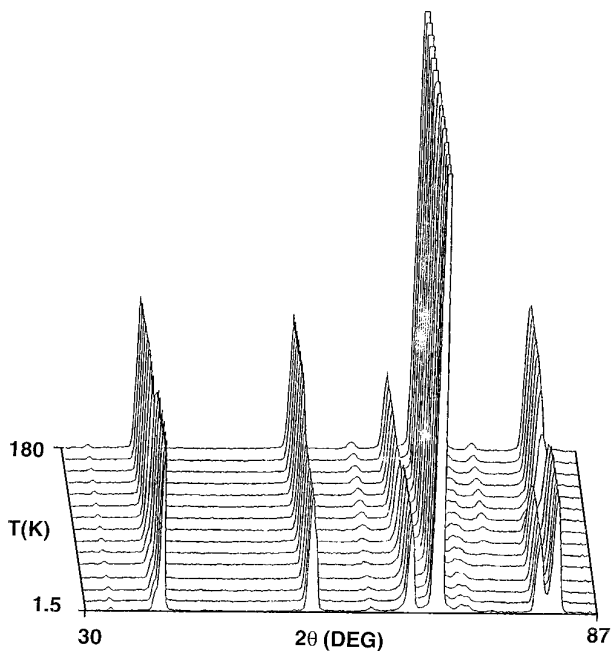

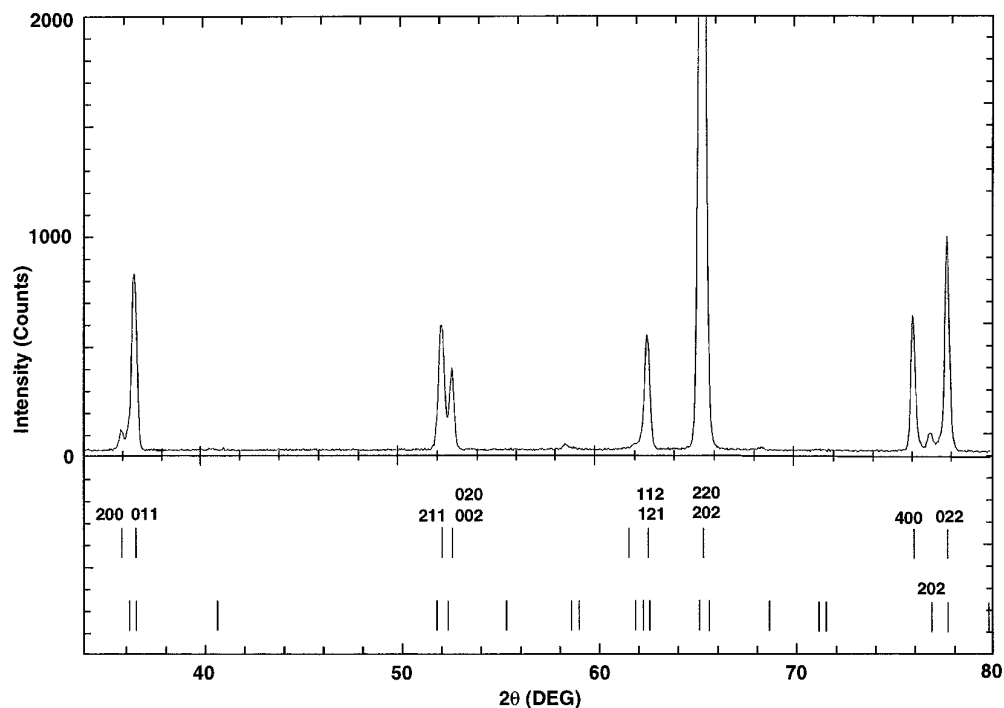**FIG. 1.** 3D-thermogram of $Pr_{0.6}Sr_{0.4}MnO_3$ between 1.5 and 180 K (D1B data).

FIG. 3. Section of the neutron diffraction pattern measured on D2B at 1.6 K, using $\lambda = 2.39$ Å. The tick marks below the spectrum indicate the calculated position of the Bragg reflections used for indexing. The upper row corresponds to a phase with $a \approx c = 5.39$ Å and $b = 7.77$ Å whereas the lower one corresponds to the high-temperature *Pnma* phase with $a = 5.46$ Å, $b = 7.66$ Å, and $c = 5.42$ Å. The most important reflections were labeled.

3. RESULTS AND DISCUSSION

Figure 1 shows part of the 3D-thermogram as measured for $Pr_{0.6}Sr_{0.4}MnO_3$ on D1B between 1.5 and 150 K. A structural phase transition takes place at about 110 K. With decreasing temperature, the nonresolved 004/220 peak at $2\Theta = 81.5°$ splits into two well-separated peaks. Peaks at $62°$ and $75°$ disappear or diminish in intensity. The system being ferromagnetic already below $T_C = 300$ K, the absence of additional peaks at low 2Θ values excludes the magnetic origin of this phase transition.

A fit of the halfwidth of the Bragg peak at $2\Theta = 55°$—comprising the $121, 200$, and 002 reflections using the *Pnma* setting—is shown in Fig. 2 and evidences the transition temperature to be $T_S = 106$ K.

Spectra above this temperature were refined using the space group *Pnma*. Below T_S, the available 2Θ range and the lack of resolution did not allow the new space group to be determined from the D1B spectra. Figure 3 shows part of the high resolution data recorded on D2B with $\lambda = 2.39$ Å. Clearly seen is the presence of two phases. One of them can still be indexed as *Pnma* with $a = 5.46$ Å, $b = 7.66$ Å, and $c = 5.42$ Å and corresponds to about 12% of the nontransformed high-temperature phase. Attempts to index the Bragg peaks belonging to the second phase

on an orthorhombic lattice yielded $a \approx c \approx 5.39$ Å and $b = 7.77$ Å. Furthermore, the extinction conditions were found to be consistent with an *I*-centered lattice.

As the a and c lattice parameters of the new phase were found to be very similar, we examined at first the possibility that the low-temperature phase had tetragonal symmetry. Based on Glazer's analysis of tilt distortions in perovskites (22) the only *I*-centered tetragonal space group with $a = b \approx \sqrt{2}a_p$ and $c \approx 2a_p$ is *I4/mcm* (No. 140). Jirak *et al.* (4) reported for $Pr_{0.65}Ba_{0.35}MnO_3$ a low-temperature phase of symmetry *I4/mcm*. Therefore, a preliminary Rietveld refinement was attempted using *I4/mcm* for the majority phase and *Pnma* for the minority phase (nontransformed high-temperature phase). However, although the calculated pattern obtained using this model reproduced qualitatively all the features of the experimental data, the goodness of fit was not completely satisfactory. As a consequence, other possible space group symmetries, allowing small distortions from the *I4/mcm* phase, needed to be taken into consideration. Using Glazer's formalism for tilt distortions, the *I4/mcm* phase is represented by the symbol $a^0a^0c^-$, indicating that the distorted phase can be obtained from the undistorted perovskite (*Pm3m*) by a simple rotation of the octahedra around the primitive perovskite $[001]_p$ direction, two adjacent layers along the c axis being
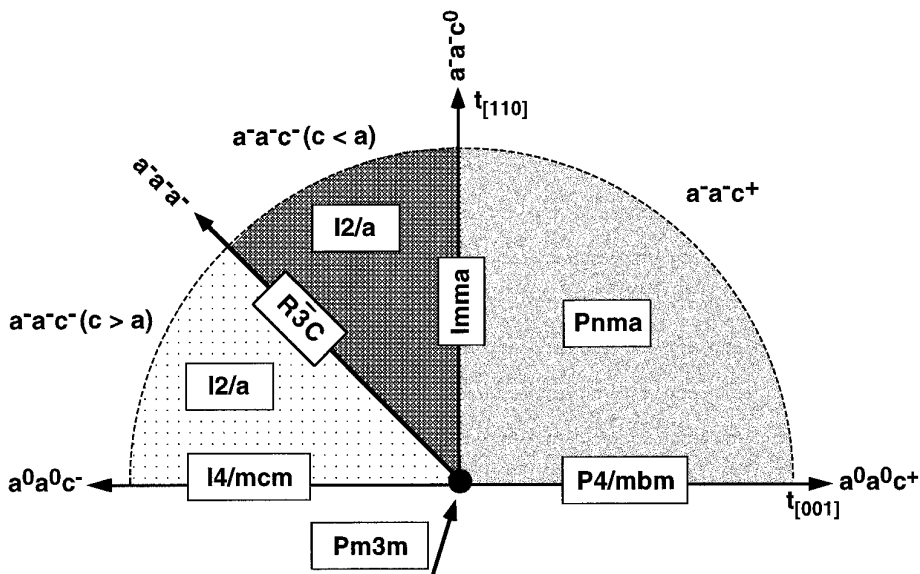
FIG. 4. Generalized phase diagram depicting the relationship between the various perovskite allotypes, using the notion of tilts as introduced by Glazer (22).
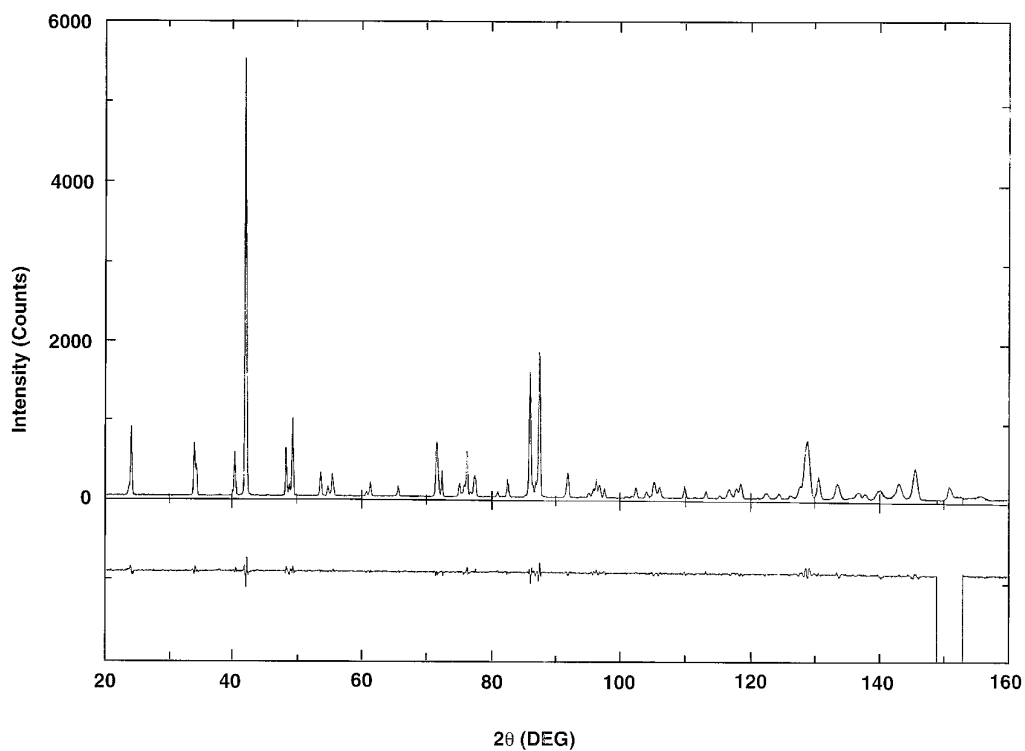

FIG. 5. Rietveld refinement plot of the neutron powder diffraction data for $Pr_{0.6}Sr_{0.4}MnO_3$ at 1.6 K and $\lambda = 1.594$ Å. The difference curve between observed and calculated profiles is plotted at the bottom.

rotated in opposite directions (antiphase tilts). With the same choice of axes, the other known phases in the system have the notations $a^-a^-c^+$ (*Pnma*), $a^-a^-a^-$ ($R\bar{3}c$), and $a^-a^-c^0$ (*Imma*), and are all characterized by the presence of two equal tilts a^-a^- along two of the primitive perovskite axes, which is equivalent to a *single* tilt around the $[110]_p$ primitive perovskite direction. Along the third perovskite axis, the tilts are in-phase for the *Pnma* phase, antiphase and equal in magnitude to the other two directions for the $R\bar{3}c$ phase, and equal to zero for the *Imma* phase. A generalized phase diagram showing the relationships between these phases is shown in Fig. 4. From the diagram, it is clear that the space group $I4/mcm$ can be obtained in a continuous way from the monoclinic space group $I2/a$ ($a^-a^-c^-$) by reducing the $[110]_p$ tilt angle to zero. This makes $I2/a$ a good candidate for the low-temperature phase. It is noteworthy that neither $I2/a$ nor $I4/mcm$ can be continuously transformed into *Pnma*, except by crossing other phase lines. Therefore, a direct phase transition from *Pnma* to one of these phases must be first order. In the light of these observations, new refinements of the structural parameters were attempted using $I2/a$ for

TABLE 1
Refined Structural and Magnetic Parameters of $Pr_{0.6}Sr_{0.4}MnO_3$ at 1.6 K

Parameter		$I2/a$ (unique axis b)	*Pnma*
Volume fraction		88%	12%
a (Å)		7.7905(1)	5.4373(3)
b (Å)		5.4038(1)	7.6721(7)
c (Å)		5.4047(2)	5.4771(4)
$\beta(°)$		90.152(1)	
Pr/Sr	x	1/4	0.011(3)
	y	−0.0016(7)	1/4
	z	0	−0.005(2)
	B	0.16(2)	0.16(2)
	M (μ_B)	0.37(3)	Not refined
Mn	x	0	0
	y	1/2	0
	z	0	1/2
	B	0.07(3)	0.07(3)
	M (μ_B)	3.39(3)	3.2, fixed
O1	x	1/4	0.494(3)
	y	0.4875(7)	1/4
	z	0	0.054(2)
	B	0.47(2)	0.47(2)
O2	x	0.4949(3)	0.269(1)
	y	0.7099(7)	0.0288(8)
	z	0.2906(7)	0.734(1)
	B	0.47(2)	0.47(2)
R_{Bragg}		3.33%	11.0%
$R_{Magnetic}$		2.32%	10.1%

Note. Numbers in parentheses are statistical errors of the last significant digits. The Debye–Waller B factors of the minority phase *Pnma* were constrained to be equal to those of the majority phase $I2/a$.

TABLE 2
Selected Structural Parameters of the $I2/a$ Phase for $Pr_{0.6}Sr_{0.4}MnO_3$ as a Function of Temperature

Parameter		1.6 K	60 K	90 K	105 K	120 K
Volume fraction		88%	87%	38%	12%	9%
a (Å)		7.7905(1)	7.7901(1)	7.7879(2)	7.7858(4)	7.7791(6)
b (Å)		5.4038(1)	5.4045(1)	5.4054(3)	5.4083(4)	5.4255(5)
c (Å)		5.4047(2)	5.4051(2)	5.4063(3)	5.4028(4)	5.4017(4)
β (°)		90.152(1)	90.143(1)	90.126(2)	90.132(5)	90.123(9)
Pr/Sr	y	−0.0016(7)	−0.0017(8)	0.000(1)	0.005(4)	0.006(5)
O1	y	0.4875(7)	0.4876(7)	0.486(1)	0.487(3)	0.471(4)
O2	x	0.4949(3)	0.4954(3)	0.4941(5)	0.490(1)	0.478(1)
	y	0.7099(7)	0.7098(7)	0.710(1)	0.711(2)	0.719(2)
	z	0.2906(7)	0.2901(7)	0.289(1)	0.288(2)	0.284(1)

Note. Numbers in parentheses are statistical errors of the last significant digits.

the majority phase. Figure 5 shows the refinement of the $\lambda = 1.59$ Å data on $Pr_{0.6}Sr_{0.4}MnO_3$ at 1.6 K using $I2/a$ as the space group for the majority phase. Comparing the resulting R values of this refinement with those of the first refinement using $I4/mcm$ a clear improvement can be observed ($\chi^2 = 6.56$ for $I4/mcm$, $\chi^2 = 2.82$ for $I2/a$).

Table 1 lists the refined structural parameters for the two phases at 1.6 K. The volume percentage of the non-transformed *Pnma* phase amounts to 12%. Small inhomogeneities in the concentration may be at the origin of this incomplete transition of the sample volume (23). For both phases the magnetic structure is, as expected for this doping level, of the simple ferromagnetic type with the moment aligned in direction of the longest axis (a axis in $I2/a$, b axis in *Pnma*). A small moment of 0.4 μ_B, parallel to the Mn moments, was found for the Pr site. The value of the magnetic moment of the minority phase was fixed to 3.2 μ_B as determined from data above T_S.

Table 2 contains the refined values of the structural parameters for the $I2/a$ phase, at the five measured temperatures. The evolution of the lattice parameters of the $I2/a$ phase and of the scale factors of the two phases as a function of temperature are shown in Fig. 6 (bottom and middle, respectively) (24). While approaching the transition, a strong decrease of the a parameter and a corresponding increase of the b parameter can be clearly observed. Figure 6 (top) shows the temperature dependence of the two tilts which define the low temperature phase $I2/a$. While the $[001]_p$ tilt (around the monoclinic a axis with our cell choice) decreases, the tilt around the $[110]_p$ axis (monoclinic c axis)—corresponding to a^-a^-—increases while approaching T_S. From these two tendencies it can be concluded (see Fig. 4) that the $I2/a$ phase is departing from $I4/mcm$ and heading toward $R\bar{3}c$. The $R\bar{3}c$
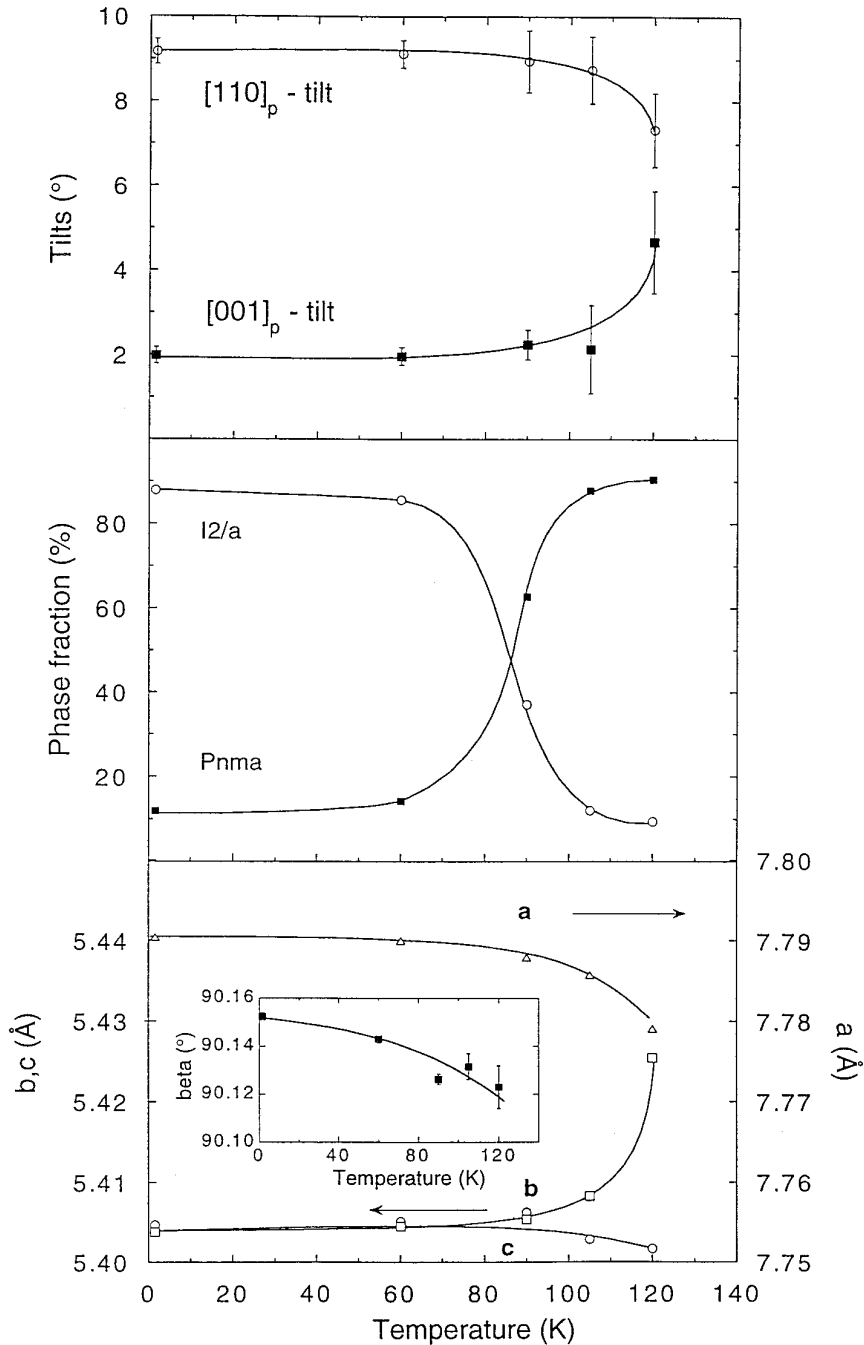
FIG. 6. (Bottom) The thermal variation of the lattice parameters in the *I2/a* phase. (Middle) The evolution of the volume fractions of the *I2/a* and the *Pnma* phases as a function of temperature. (Top) Thermal variation of the two tilts defining the perovskite allotype with *I2/a* symmetry. For more details see text.

phase itself is, however, never observed, the transition to the *Pnma* phase being first order.

4. CONCLUSIONS

Using neutron powder diffraction data we have evidenced the presence of a new *I2/a* allotype of the perovskite structure in the $(R_{1-x}A_x)$MnO$_3$ system. A structural phase transition from *Pnma* to *I2/a* was found to occur at $T_S = 105$ K for Pr$_{0.6}$Sr$_{0.4}$MnO$_3$, which has an average A site ionic radius $\langle r_A \rangle = 1.23$. This value corresponds to a tolerance factor $t = 0.931$. The *I2/a* phase is absent in the phase diagram proposed by Radaelli *et al.* for the $x = 0.3$ doping level, where compounds with $t = 0.931$ have $R\bar{3}c$

symmetry. We therefore conclude that, at constant values of the tolerance factor, phase stability is directly affected by electronic doping. This leads to a remarkably complex phase diagram, in which both structural and electronic properties are established by the interplay between doping and steric effects.

REFERENCES

1. E. O. Wollan and W. C. Koehler, *Phys. Rev.* **100,** 545 (1955).
2. Z. Jirák, S. Krupicka, V. Nekvasil, E. Pollert, G. Villeneuve, and F. Zounova, *J. Magn. Magn. Mater.* **15–18,** 519 (1980).
3. Z. Jirák, S. Krupicka, Z. Simsa, M. Dlouhá, and S. Vratislav, *J. Magn. Magn. Mater.* **53,** 153 (1985).
4. Z. Jirák, E. Pollert, A. F. Andresen, J. C. Grenier, and P. Hagenmuller, *Eur. J. Solid State Inorg. Chem.* **27,** 421 (1990).
5. K. Knízer, Z. Jirák, E. Pollert, F. Zounova, and S. Vratislav, *J. Solid State Chem.* **100,** 292 (1992).
6. C. Zener, *Phys. Rev.* **82,** 403 (1951).
7. R. M. Kusters, J. Singleton, D. A. Keen, R. McGreevy, and W. Hayes, *Physica B* **155,** 362 (1989).
8. R. von Helmolt, J. Wecker, B. Holzapfel, L. Schultz, and K. Samwer, *Phys. Rev. Lett.* **71,** 2331 (1993).
9. K. Chahara, T. Ohno, M. Kasai, and Y. Kozono, *Appl. Phys. Lett.* **63,** 1190 (1993).
10. S. Jin, T. H. Tiefel, M. McCormack, and R. A. Fastnacht, *Science* **264,** 413 (1994).
11. Y. Tomioka, A. Asamitsu, Y. Moritomo, H. Kuwahara, and Y. Tokura, *Phys. Rev. Lett.* **74,** 5108 (1995).
12. H. Yoshizawa, H. Kawano, Y. Tomioka, and Y. Tokura, *Phys. Rev. B* **52,** 13145 (1995).
13. M. R. Lees, J. Barratt, G. Balakrishnan, and D. Mc. K. Paul, *Phys. Rev. B* **52,** 14303 (1995).
14. A. J. Millis, P. B. Littlewood, and B. I. Shraiman, *Phys. Rev. Lett.* **74,** 5144 (1995).
15. J. M. De Teresa, M. R. Ibarra, J. Blasco, J. García, C. Marquina, and P. A. Algarabel, *Phys. Rev. B* **54,** 1187 (1996).
16. A. J. Millis, B. I. Shraiman and R. Mueller, *Phys. Rev. Lett.* **77,** 175 (1996).
17. H. Y. Hwang, S.-W. Cheong, P. G. Radaelli, M. Marezio, and B. Batlogg, *Phys. Rev. Lett.* **75,** 914 (1995).
18. P. G. Radaelli, M. Marezio, H. Y. Hwang, and S.-W. Cheong, *J. Solid State Chem.* **122,** 444 (1996).
19. V. M. Goldschmidt, *Mat.-Naturv.Kl.* **2,** 117 (1926).
20. J. M. De Teresa, M. R. Ibarra, J. Garcia, J. Blasco, C. Ritter, P. A. Algarabel, C. Marquina, and A. del Moral, *Phys. Rev. Lett.* **76,** 3392 (1996).
21. J. Rodríguez-Carvajal, M. Anne, and J. Pannetier, unpublished.
22. A. M. Glazer, *Acta Crystallogr. A* **31,** 756 (1975).
23. Unpublished data of the authors on $Pr_{0.6}Sr_{0.38}Ca_{0.02}MnO_3$ show that the volume percentage of the $I2/a$ phase at 1.5 K has already dropped to about 30%.
24. The halfwidth of the Bragg peak which was used to determine the transition temperature is changing as the relative fractions of $I2/a$ and *Pnma* phases are changing. Using the temperature dependent data of D1B a significant decrease of the linewidth is detectable until about 105 K. The high resolution data of D2B showed that at this temperature 12% of the volume sample is still in the $I2/a$ phase. At 120 K this percentage has dropped only to 9% (see Table 2). This explains why no significant decrease of the linewidth was found above about 105 K.